NASA
TP
1487
c.1

TECH LIBRARY KAFB, NM
0134669

LOAN COPY: RETUR
AFWL TECHNICAL
KIRTLAND AFB, N.

NASA Technical Paper 1487

Axial Jet Mixing of Ethanol in Cylindrical Containers During Weightlessness

John C. Aydelott

JULY 1979

NASA

TECH LIBRARY KAFB, NM
0134669

NASA Technical Paper 1487

Axial Jet Mixing of Ethanol in Cylindrical Containers During Weightlessness

John C. Aydelott
Lewis Research Center
Cleveland, Ohio

National Aeronautics
and Space Administration

**Scientific and Technical
Information Branch**

1979

SUMMARY

An experimental program was conducted in the 5-second mode of the Lewis Research Center's 5- to 10-second zero-gravity facility to examine the liquid flow patterns that result from the axial jet mixing of ethanol in 10-centimeter-diameter cylindrical containers in weightlessness. Three cylindrical tank configurations were used for the study: a convex hemispherically ended container; and two Centaur liquid-hydrogen-tank models, one with slosh baffles and one without. Four distinct liquid flow patterns were observed: dissipation of the liquid jet in the bulk-liquid region, geyser formation, liquid collection at the end of the tank opposite the jet exit, and complete circulation of the liquid along the tank walls. The transition between flow patterns was a function of the tank geometry, the liquid-jet velocity, the volume of liquid in the tank, and the location of the tube from which the liquid jet exited. Several tests were also conducted under normal-gravity conditions for comparison.

INTRODUCTION

The use of cryogenic propellants in the NASA space program has introduced problems of propellant management (ref. 1). During missions in space, cryogenic propellant tanks will require periodic venting, as the tank pressure increases as a result of various heat inputs, to keep the tank pressure within acceptable limits. Currently, orbiting propellant tanks are vented by using settling rockets to position and maintain the liquid away from the vent and thus to permit the direct venting of only vapor from the tank.

Efforts to improve the performance of propulsive stages have introduced the concept of the thermodynamic vent system, a lighter weight method of controlling tank pressure than liquid settling and direct venting (ref. 2). In the thermodynamic vent system, a small amount of the cryogenic propellant is evaporated to offset the unavoidable heat addition to the propellant tank. Cryogenic liquid is withdrawn from the tank and passed through a Joule-Thompson valve with a resultant pressure and temperature reduction. This cold, two-phase fluid is then introduced into a heat exchanger, where evaporation continues and heat absorption takes place before the resulting vapor is vented overboard.

The heat exchanger can be located within the tankage insulation, on the tank wall, or inside the propellant tank. In the first option, most of the incoming heat is intercepted before it reaches the propellant. In the third option, the cryogenic liquid and vapor in

the propellant tank are the heat-exchanger hot-side fluid. This fluid is cooled during operation of the thermodynamic vent system, thus reducing the tank pressure. In the second option, locating the heat exchanger on the tank wall, partial heat interception is combined with propellant tank cooling to control tank pressure.

The third option - commonly called an internal, compact heat exchanger - should have the lowest weight, but it introduces the additional requirement of circulating the fluid in the tank so that effective cooling can take place. However, circulating, or mixing, the bulk cryogenic liquid does simplify orbital propellant management. The tank pressure rises more slowly because temperature stratification of the liquid and vapor does not develop, and there are fewer problems with engine startup because a uniform temperature and density liquid is delivered to the engine feedlines.

Thermodynamic vent system concepts are particularly attractive when cryogenic payloads for the Space Shuttle are considered. Under many normal operating conditions and all abort modes, payload requirements cannot dictate Shuttle operations, so settling to relieve the payload tank pressure would be impossible. Thermodynamic vent systems should impose no operating constraints on the Space Shuttle.

Thermodynamic vent systems with internal, compact heat exchangers and mixers have been designed, fabricated, and tested in cryogenic fluids under normal-gravity conditions (ref. 3). The ability of these devices to control tank pressure at 1 g has led to their general acceptance as the planned pressure control technique for the Orbital Transfer Vehicle and other future cryogenic tankage designed for weightless operation.

Although the analytical technique for designing the internal, compact heat exchanger has not been verified experimentally under low-gravity conditions, its performance should not vary significantly with gravity level. However, the fluid dynamics necessary to mix the bulk fluid in a predictable manner depend highly on the acceleration level (ref. 4). The difference between normal gravity and weightlessness will influence not only the liquid-vapor configuration before mixing, but also the liquid momentum or velocity required to establish the desired liquid flow pattern and degree of mixing.

In an earlier study (ref. 4) the author examined the liquid flow patterns that resulted when an axial liquid jet (a circular liquid jet directed along the axis of the container) was used to mix ethanol in a 10-centimeter-diameter spherical container in weightlessness. The effects of the liquid volume in the tank, the position of the liquid-jet outlet, and the liquid-jet inflow rate on the resulting liquid flow patterns were examined. At liquid fillings by volume of 50 percent or less, complete liquid circulation was easily established. At liquid fillings by volume of 70 percent or more, vapor was drawn into the inlet of the simulated mixer. Increasing the liquid-jet velocity to avoid vapor ingestion made the tank contents highly turbulent, with bubbles becoming entrained in the bulk liquid. Uniform liquid flow patterns were easier to achieve when the liquid jet exited near the top of the container rather than at the bottom.

The experimental program reported herein was conducted to examine the flow patterns that resulted when an axial liquid jet was used to mix the contents of partially filled cylindrical containers. The objective of the program was to define the jet characteristics required to effectively mix the liquid without bubble formation or excessive turbulence. The liquid mixing, or circulating, processes should adequately intercept the heat entering a cryogenic propellant tank and thus effectively control the tank pressure.

Three 10-centimeter-diameter cylindrical tank configurations were used in the study: (1) tank A - a convex hemispherically ended cylindrical tank with a length-diameter ratio of 2 (fig. 1(a)); (2) tank B - a Centaur liquid-hydrogen-tank model with one convex hemispherical end, one concave ellipsoidal end, and no slosh baffles (fig. 1(b)); and (3) tank C - a similar Centaur liquid-hydrogen-tank model but with internal slosh baffles at the 30- and 77-percent liquid fill levels. A piston pump with a 0.4-centimeter-diameter exit tube was located in the convex hemispherical end of each tank. Liquid was withdrawn from the tank at the base of the exit tube as liquid was forced into the tank through the tube as an axial jet. This process simulated the liquid flow pattern associated with a pump in the forward end of the tank. The forward end of the tank was chosen as the pump location because under Earth-orbiting conditions liquid would be positioned over the pump as a result of the acceleration caused by atmospheric drag.

Of equal importance with observing liquid flow patterns was examining the motion of the ullage, or main vapor region. Vapor encapsulation of the simulated pump (i.e., vapor ingested in the region of fluid withdrawal) would lead to failure of the liquid circulation concept. The effects on the liquid flow patterns of initial liquid filling, jet outlet position, and liquid-jet velocity were examined at both normal and zero gravity.

BACKGROUND

Liquid-Jet Mixing of Fluids

Analytical studies performed to determine the best way to mix fluid in cryogenic tankage (ref. 5) have shown that radial and axial liquid-jet pumps (fig. 2) are the most promising devices. The liquid leaves an axial jet pump as a single fluid stream generally flowing along the tank centerline while liquid is uniformly drawn into the pump around the base. The liquid flow pattern associated with a radial jet pump is the exact opposite: Liquid flows radially outward from the base of the pump and is returned to the pump from the center of the tank.

Comparison of axial and radial liquid-jet pumps. - Either axial or radial liquid-jet pumps appear acceptable for bulk-liquid mixing in cylindrical tanks. The bulk liquid

would have a preferred location because of surface tension forces, even under weightless conditions. However, mixing only the bulk liquid, which is desirable for minimizing the disturbing forces on the vehicle, can lead to inadequate pressure control since vapor cooling would depend solely on the heat and mass transfer taking place at the liquid-vapor interface. Therefore, it may be necessary to flow liquid over the entire cylindrical tank wall to provide cooling and the desired pressure response.

An experimental study of the effect of gravity on forced liquid circulation patterns in spherical tanks was conducted at Lewis (ref. 6). The liquid flow pattern resulting from a radial jet was experimentally observed in three different size tanks at acceleration levels from normal gravity to essentially zero gravity. For an initially empty tank and radial jet inlet velocities great enough to cause liquid flow up the walls and down the center of the tank, a great deal of turbulence, unsymmetric flow, and bubble formation resulted. Bubble formation defeats one of the advantages of the thermodynamic vent system concept: the delivery of a uniform temperature and density liquid to the engine feedlines. Turbulent and unsymmetric liquid flow can add excessive demands to vehicle or spacecraft attitude-control systems.

Axial jets are preferred if it is desired to totally wet the tank walls under weightless conditions. This complete-circulation liquid flow pattern results when the liquid jet impinges on the top, or aft end, of the tank. The liquid then flows along the tank walls to the interface between the bulk liquid and the vapor, and liquid is drawn into the pump at the bottom, or forward end, of the tank.

Effect of liquid depth over pump outlet. - The position of the outlet for an axial liquid jet, relative to the bulk liquid-vapor interface, greatly affects the resulting jet characteristics. According to the classical theory for the behavior of axial jets flowing through a fluid (ref. 7), a submerged jet maintains nearly constant momentum as it progresses from the outlet. As the jet flows through the bulk liquid, its mass flow rate increases, because of bulk-liquid entrainment, and its average velocity decreases because of radial momentum transport by viscous effects. Consequently, for axial jets with outlets positioned in the bulk liquid, increasing the liquid filling in the tank will increase the size and mass flow rate of the liquid jet and reduce its average velocity at the liquid-vapor interface.

The jet outlet position and tank filling are not the only parameters that determine the depth of bulk liquid that the liquid jet must penetrate. Under weightless conditions the liquid-vapor interface becomes hemispherical (fig. 2) and thus liquid depth over the jet exit is less than with the same tank filling under normal gravity. Two exceptions to this occur in the baffled Centaur model tank. For tank liquid fillings of approximately 30 and 70 percent the lower and upper slosh baffles, respectively, restrict the motion of the liquid-vapor interface so that the highly curved zero-gravity configuration typical

of unbaffled tanks does not occur. Consequently, the liquid depth over the jet exit was greater for these test conditions than for the corresponding tests in the unbaffled tanks.

Liquid-Jet Velocity Requirements

Determination of the minimum required axial liquid-jet velocity for establishing the bulk-liquid mixing flow pattern was based on a Lewis study of liquid inflow to partially filled tanks (ref. 8). That program determined the maximum liquid inflow rate such that stable filling (minimum liquid-vapor interface distortion) of the container resulted. Based on this criterion, zero-gravity filling of the 10-centimeter-diameter test container would be stable if the inflow rate was no greater than approximately 2.4 cubic centimeters per second. A minimum inflow rate of approximately 2 cubic centimeters per second was chosen for this study to provide the bulk-liquid mixing flow pattern.

Higher liquid-jet inflow rates of approximately 3, 4, 6, 8, 12, 16, 24, and 36 cubic centimeters per second were selected to allow study of the complete-circulation liquid flow pattern. The maximum inflow rate was based on the author's earlier work (ref. 4), which indicated that undesirable, highly turbulent flow patterns result at inflow rates from 24 to 48 cubic centimeters per second.

APPARATUS AND PROCEDURE

The Lewis zero-gravity facility was used to obtain the experimental data for this investigation. The facility, the experiment package, and the procedure for conducting the tests are described completely in the appendix.

A schematic drawing of the liquid flow system is shown in figure 3. A piston pump, driven by an electric motor and gear mechanism, forces the ethanol test liquid out through the central tube and forms an axial liquid jet. Simultaneously, liquid is withdrawn from the bottom of the experiment tank and fills the region below the piston pump. Interchangeable liquid-jet exit tubes of different lengths could be fit into the opening at the top of the piston pump.

The speed of the piston pump, and thus the liquid-jet volumetric flow rate, is controlled by various combinations of gear drives and applied voltage to the electric motor. As the piston moves, an electrical contact slides along a linear resistor mounted parallel to the piston pump. A 28-volt, direct-current circuit, including the linear resistor that acts as a voltage divider, provides the input to a telemetry system that transmits to a receiver and strip-chart recorder in the facility control room so that the position of the piston pump as a function of time can be determined. Because the piston drive mechanism occupies approximately 30 percent of the piston sleeve volume, the

liquid volumetric withdrawal rate is only 70 percent of the liquid-jet volumetric flow rate.

During a test under weightless conditions, the first 2 seconds of test time were allocated for the bulk liquid to achieve a zero-gravity configuration. The liquid flow system was then activated by timers for the remaining test time, 3.1 seconds. For simplicity, the same sequence and timing of operations were used for the normal-gravity tests.

A high-speed motion-picture camera was used to photograph the bulk-liquid motion during the first 2 seconds of test time and the liquid flow patterns within the cylindrical experiment tanks after the piston pump was activated. The liquid jet was dyed to clarify the liquid flow patterns. A digital clock was included in the camera field of view so that the elapsed time from the start of the test would be recorded.

TEST PARAMETERS

The experimental conditions for the 22 normal-gravity tests and the 74 zero-gravity tests ($<10^{-5}$ g's), together with the characteristics of the axial liquid jet for each test are presented in table I. The three 10-centimeter-diameter experiment tank configurations are designated by the letters A - convex hemispherically ended cylindrical tank with a length-diameter ratio of 2 and a volume of 1310 cubic centimeters; B - a Centaur liquid-hydrogen-tank model with one convex hemispherical end, one concave ellipsoidal end, no slosh baffles, a length-diameter ratio of 2, and a volume of 1270 cubic centimeters; C - a similar Centaur liquid-hydrogen-tank model that included internal slosh baffles at the 30- and 77-percent liquid fill levels. Other experimental variables were initial experiment tank liquid fillings of approximately 30, 50, 70, and 90 percent (by volume), two outlet positions for the axial liquid jet, and the piston pump velocity.

The lengths of the axial jet exit tubes, 1 and 8 centimeters, were measured from the hypothetical bottom of each experiment tank. For each test the average piston pump velocity was determined from the position-versus-time trace obtained from the strip-chart recorder. The average piston pump velocity was multiplied by the piston cross-sectional area to obtain the liquid-jet volumetric flow rate. The liquid-jet volumetric flow rate was divided by the cross-sectional area of the jet exit tube to yield the average liquid-jet velocity. The jet volumetric flow rate was also divided by the tank volume and multiplied by the 3.1-second test time to obtain the percentage of the tank volume that flows into the tank as a liquid jet during each test. This normalized liquid-jet volumetric flow rate (table I) was the most suitable parameter for describing the fluid flow phenomena discussed in later sections. For simplicity, this normalized liquid-jet volumetric flow rate is referred to as the inflow rate and is expressed in units of

percent. The fact that the liquid withdrawal rate from the container was approximately 30 percent less than the inflow rate probably affected only the experimentally determined bulk-liquid mixing rates. The other test results and general conclusions should be unaffected since, for all test conditions, the container liquid filling during the test increased by less than 3 percent.

TEST RESULTS

Four distinct liquid flow patterns were observed during testing under weightless conditions:

(1) Pattern I - dissipation of the liquid jet in the bulk-liquid region

(2) Pattern II - geyser formation

(3) Pattern III - collection of jet liquid in the aft end of the tank (opposite the jet exit)

(4) Pattern IV - liquid circulation over the aft end of the tank and down the tank wall

Liquid flow patterns I, II, and IV were observed during testing under normal-gravity conditions. The resulting liquid flow pattern for each test is identified by these Roman numerals in table I.

The time required, after the piston pump began to move, for complete bulk-liquid mixing (pattern I or IV) and liquid circulation (pattern IV) was either measured or extrapolated from the data for each test. The measured bulk-liquid mixing times are the times required for the bulk liquid to become completely dyed by the incoming liquid jet. The measured liquid circulation times are the times required for the liquid from the jet to flow over the aft end of the tank and down that portion of the tank wall that was initially dry.

For bulk-liquid mixing, the extrapolation technique involved measuring the position of the demarcation line between the dyed and undyed liquids in the bulk-liquid region as a function of time. From these measurements the velocity of the demarcation line between the dyed and undyed liquids was determined and multiplied by the tank cross-sectional area to establish the bulk-liquid mixing rate. The volume of unmixed liquid bulk at the end of each test was then divided by this experimentally determined mixing rate, and the resulting time increment was added to the test time to obtain an estimate of the time required for complete bulk mixing.

For test conditions that would have yielded a complete-circulation liquid flow pattern, given enough test time, the velocity of the liquid front flowing down the tank wall was determined. A linear extrapolation technique was then used, based on this experimentally determined liquid-front velocity, to project the total time required for the liquid front to completely wet the dry tank wall.

The bulk-liquid mixing and complete liquid circulation times determined from the test measurements (3.1 sec or less) and from the analytical extrapolations (greater than 3.1 sec) are also given in table I.

DISCUSSION OF TEST RESULTS

Symmetric Liquid Flow Patterns

Pattern I - dissipation of the liquid jet in the bulk-liquid region. - At the lowest inflow rates tested the axial liquid jet entered the tank as a thin laminar stream under both normal-gravity and weightless conditions. Figures 4(a) and (b) show the results for test 14, which was conducted at normal gravity with an inflow rate of 0.5 percent. The thin laminar jet rose to the liquid-vapor interface and the dyed liquid spread across the interface, yielding an orderly mixing of the bulk liquid in a region that progressed downward with time.

Figure 5 presents the results for test 16, which was conducted under weightless conditions at an inflow rate of 0.7 percent. The slightly greater inflow rate than for test 14 caused the liquid jet to diffuse somewhat into the bulk-liquid region, indicating a transition from laminar to turbulent flow. As in figures 4(a) and (b), the dyed liquid collected in the liquid-vapor interface region and mixing of the liquid bulk progressed downward with increasing time. The most significant difference between normal-gravity and weightless testing that can be observed by comparing figures 4(b) and 5(c) is the highly irregular liquid-vapor interface that resulted from operation of the liquid jet in zero gravity.

Under normal-gravity conditions, for the tests with the 1-centimeter-long jet exit tube, liquid flow pattern I existed for inflow rates to approximately 6 percent. The results of test 45 (fig. 4(c)) are typical of the results of these tests after several seconds. Spreading and dissipation of the liquid jet in the central bulk-liquid region was quite apparent; however, the dyed liquid still collected at the liquid-vapor interface, and progressive downward mixing of the liquid bulk resulted.

Pattern II - geyser formation. - Increasing the inflow rate or raising the position of the liquid-jet outlet caused a geyser to form in the central region of the test tank. Under normal-gravity conditions this geyser looked like a fountain with the liquid jet rising above the bulk liquid-vapor interface and falling back into the central bulk-liquid region (fig. 6). Consequently, the liquid dye was concentrated in the central region of the test tank and complete mixing of the liquid bulk was not accomplished. In particular, most of the bulk liquid near the tank wall remained undyed. The heat addition to a cyogenic propellant tank would be primarily through the tank walls so that this liquid flow

pattern would be ineffective in reducing temperature gradients and providing pressure control.

In zero gravity the geysers continued to grow with time in the ullage region of the experiment tanks. Test 24 (fig. 7) was typical of the six tests (tests 2, 24, 25, 80, 81, and 92) that yielded this phenomenon. For these tests the spreading and diffusion of the liquid jet did cause some bulk-liquid mixing, but the formation of the large liquid globule in the center of the tank was the significant feature. The ultimate liquid-vapor configuration, given enough zero-gravity test time, could not be predicted for these test conditions.

Pattern III - collection of jet liquid in the aft end of the tank. - Figures 6 and 8 show the effect of changing from normal to zero gravity for otherwise identical test conditions. In weightlessness (fig. 8) the liquid jet impinged on the concave aft end, or bulkhead, of the Centaur model tank, rather than falling back into the bulk-liquid region (fig. 6), and the jet liquid then collected in the crevice formed by the intersection of the tank sides and the bulkhead.

Obviously, under normal-gravity conditions, no set of experimental parameters would lead to liquid flow pattern III. It also appears that tank shape A, which has convex hemispherical ends, will exhibit this liquid flow pattern only over a very narrow range of inflow conditions. Test 18, which used a central jet exit position, yielded a liquid flow pattern that appeared to be on the verge of transition to pattern IV at an inflow rate of only 0.7 percent. Tests 24 and 32 reveal that liquid flow pattern III was completely bypassed, for a low jet exit position, in going from an inflow rate of 1.5 percent to a rate of 2.1 percent.

The conclusion to be drawn from this discussion is that the concave bulkhead, and the resulting crevice in the tank wall in the Centaur model tanks, is more conducive to the formation of liquid flow pattern III than is the concave bulkhead. The tortuous flow path required of the liquid-jet fluid by this geometry probably dissipated the momentum of the jet, and thus the liquid collected at the opposite end of the tank from the jet outlet. More discussion concerning the nature and extent of this flow regime is presented in succeeding sections.

Pattern IV - liquid circulation over the aft end of the tank and down the tank wall. - Further increasing the inflow rate resulted in sufficient liquid-jet momentum to cause the liquid jet to flow over the tank end opposite the jet exit and down the tank walls to the liquid-vapor interface (fig. 9). The dyed liquid then flowed along the liquid-vapor interface and collected on top of the bulk-liquid region. As liquid was withdrawn from the tank to feed the simulated mixer the mixed bulk-liquid region moved downward, ultimately yielding a completely mixed liquid bulk.

In zero gravity, for the tests conducted with the 8-centimeter-long jet exit tube, the Centaur model tanks required higher inflow rates to establish liquid flow pattern IV

than did the test tank with convex hemispherical ends. The slosh baffles in the Centaur model tank impeded the flow of liquid down the tank walls but apparently did not affect the inflow rate required to cause a transition from pattern III to pattern IV. Under normal-gravity conditions, flow pattern IV could only be established with the 8-centimeter-long jet exit tube and a liquid-jet inflow rate greater than 8 percent.

Undesirable Liquid Flow Conditions

The results from a few zero-gravity tests do not fit into the previously discussed liquid flow pattern classifications. At tank fillings of 90 percent and greater (tests 93 to 96), the vapor bubble tended to become detached from the tank wall and unsymmetric liquid flow developed (fig. 10). The ultimate position of the vapor bubble, given enough zero-gravity test time, cannot be predicted; however, the vapor bubble could drift to a position over the inlet to the simulated mixer. Ingestion of vapor by the mixer would lead to failure of the liquid circulation concept. This behavior is similar to the results of the high-liquid-filling tests presented in reference 4 for spherical containers.

At inflow rates greater than 8 percent the liquid flow pattern became irregular (fig. 11). These high inflow rates caused bubbles to be entrained in the bulk liquid and thus defeated the objective of providing a liquid bulk of uniform temperature and density. In addition, the liquid flow down the tank wall was occasionally entrained by the liquid jet so that some of the liquid recirculated in the vapor region of the tank (tests 70 and 72). For one test (90), at a tank filling of 74 percent and an inflow rate of 5.9 percent, the recirculation of the liquid flowing down the tank walls was so complete that negligible bulk mixing resulted.

Transitions Between Liquid Flow Patterns

The discussion thus far has indicated that the liquid-jet inflow rate and the gravitational environment were the dominant experimental parameters that determined the liquid flow patterns in the experiment tanks. In addition, the effects of liquid filling, tank shape, and jet outlet position on the liquid flow patterns were examined.

Effect of liquid filling. - Figure 12(a) shows the jet inflow rate as a function of the tank liquid filling for all the zero-gravity data obtained with the 1-centimeter-long jet exit tube. Different symbols are used to indicate the experimental data points for each of the four liquid flow patterns. The data are plotted without regard to tank shape since no effect of tank shape on the inflow rates required to establish the different flow patterns was detected for the short-jet-exit-tube tests. However, the time required for flow pattern IV to develop in the Centaur model tanks was longer than that required in the convex hemispherically ended tank.

At liquid fillings of 50 percent and more, the increasing depth of liquid over the jet outlet did not seem to have any effect. Only at nominal tank fillings of 30 percent, where the liquid depth over the jet outlet was lowest, was an effect of initial liquid filling level evident. Apparently, at low liquid fillings the energy of the liquid jet dissipated very little from its passage through the liquid bulk, so the transitions between the four liquid flow patterns occurred at lower inflow rates.

Effect of jet outlet position and tank shape. - When the liquid-jet outlet position was raised to a nearly central location (8-cm-long jet exit tube) only liquid flow patterns III and IV resulted under weightless conditions, and the effect of tank shape became significant (fig. 12(b)). For these test conditions and tank fillings of 30 and 50 percent, the jet outlet was unsubmerged. For tank shape A, convex hemispherically ended, the transition from pattern III to pattern IV occurred at a much lower inflow rate with the longer tube. However, for the Centaur model tanks the transition from pattern III to pattern IV occurred at an inflow rate nearly two times greater than the transition inflow rate with the shorter tube (fig. 12(a)). As discussed in the section BACKGROUND, the test results shown in figure 12 can be explained on the basis of an unsubmerged, higher velocity liquid jet being more effective in flowing over the smooth contours of the convex hemispherically ended tank. The higher mass-flow-rate liquid jet that resulted when the jet outlet was submerged was more effective in filling the crevice between the tank wall and the concave hemispherical end of the Centaur model tanks. Once the crevice was filled, the time required being less for a high-mass-flow-rate jet, the Centaur model tanks took on the appearance of a nearly convex hemispherically ended tank and the transition to flow pattern IV took place. This behavior suggests that flow pattern III in the Centaur model tanks may be only transient. However, the limited test time available in the Lewis zero-gravity facility did not allow resolution of this question.

Determination of Bulk-Liquid Mixing Time

The time required, after liquid-jet inflow was begun, for the dye from the liquid jet to completely mix with the bulk liquid was either measured or estimated by extrapolation of the data, as previously discussed in the section TEST RESULTS. Observing dye penetration into the bulk liquid is only an approximate measure of the real parameters of interest - bulk-liquid mixing and the destruction of thermal gradients. In addition, the difference between the 30 percent smaller liquid withdrawal rate and the liquid-jet inflow rate should have caused the observed bulk-liquid mixing times, based on dye penetration, to be shorter than those for an actual mixer with equal input and output flow rates. Consequently, emphasis should be placed not on the absolute bulk-liquid mixing times, but on the general comparisons presented.

Each test that exhibited either liquid flow pattern I or IV, that was long enough to yield meaningful data, and that had symmetric liquid flow was evaluated. The results of this data collection and analysis for all the nominal 50-percent-liquid-filling and 1-centimeter-long-jet-exit-tube tests are plotted in figure 13. The normal-gravity results are all for inflow pattern I. Under weightless conditions, both inflow patterns I and IV led to measurable rates of bulk mixing.

Comparison of normal- and zero-gravity results. - Extrapolating test results to predict the effect of increased test time is generally questionable; however, two fairly significant conclusions can be drawn from this analysis. First, for bulk mixing times of approximately 4 seconds or less (minimum extrapolation), the data for flow pattern I in normal gravity were compared with those for flow pattern IV in weightlessness for a given inflow rate (fig. 13). The difference in the bulk mixing times between the normal- and zero-gravity data was due to the time required for the liquid jet to flow over the aft end of the tank and down the tank walls under weightless conditions (complete-circulation time, table I). Even though the liquid flow patterns in normal gravity and weightlessness were completely different, the rates of bulk mixing (see section TEST RESULTS) were nearly identical once the jet liquid reached the liquid-vapor interface.

Second, the rate of bulk-liquid mixing resulting from flow pattern I under weightlessness (table II) was nearly constant for a given liquid-jet inflow rate. The results from four tests for three tank liquid fillings and two inflow rates were examined. For each test the rate of bulk-liquid mixing was divided by the inflow rate. Diffusion and turbulent mixing caused the volume of affected bulk liquid to be approximately nine times the volume of the incoming liquid jet for all four tests.

Effect of jet outlet position. - A few data points that yielded bulk mixing time information were obtained with the 8-centimeter-long jet exit tube in the convex hemispherically ended tank. Under normal-gravity conditions the measured bulk mixing time (2.9 sec at an inflow rate of 8.4 percent for test 73) would nearly fall on an extension of the figure 13 plot of the zero-gravity, flow-pattern-IV test data. Since test 73 also yielded complete liquid circulation (flow pattern IV), we might have concluded that, at liquid-jet velocities approaching 300 centimeters per second, the effects of gravity are negligible. However, test 72, conducted under weightless conditions for the same tank filling and liquid-jet inflow conditions as test 73, exhibited recirculation of the liquid flowing down the tank walls, and only half of the liquid bulk was dyed at the end of the test. It is, therefore, apparent that at inflow rates above 6 percent (for tank A and a central jet exit position) the resulting normal- and zero-gravity liquid flow conditions are not similar and that bulk mixing times are much greater under weightless conditions.

Test 75 was also conducted in normal gravity with the Centaur model tank and test conditions similar to those of test 73. The liquid flow pattern that resulted, although identified as IV in table I, was not uniform like that of test 73. When the liquid jet impinged on the concave end of the Centaur model tank, part of the liquid flow continued along the bulkhead and tank wall while the rest broke up into droplets and fell back into the bulk-liquid region, thus causing the more rapid mixing of the bulk-liquid region that was observed (table I).

The only test conducted under weightless conditions with an unsubmerged jet that had enough bulk-liquid mixing to allow analysis was test 74. The extrapolation yielded a predicted bulk mixing time of 6.0 seconds for these test conditions. This long mixing time, as compared with the submerged liquid-jet data plotted in figure 13, is due to the low mass flow rate of the unsubmerged jet. This increased the liquid circulation time and decreased the rate at which dyed fluid was delivered to the bulk-liquid region. This hypothesis is reinforced by the results of test 87, which was conducted under weightless conditions in the same tank as test 74. Test 87 was for a higher liquid filling, so the 8-centimeter-long liquid-jet exit tube was submerged and the inflow rate was approximately one-half the inflow rate for test 74. The bulk mixing time, based on extrapolation, for test 87 was 7.1 seconds, only slightly greater than the test 74 mixing time, even though more bulk liquid had to be mixed and the inflow rate had been greatly reduced.

Determination of Liquid Circulation Time

The time required after the start of liquid-jet inflow for complete liquid circulation (flow pattern IV) was either measured or extrapolated (see section TEST RESULTS) from the data for each test where the liquid circulation phenomena was observed.

Unbaffled Centaur model tank. - The data collected and extrapolated for the unbaffled Centaur model tank are plotted in figure 14. The liquid circulation times increased with decreasing inflow rate, as would be expected. In addition, for the tests conducted with the 1-centimeter-long jet exit tube, the increase in the liquid circulation time with decreasing liquid filling could have been anticipated since the liquid circulation path length along the tank wall increased with lower liquid filling. Also, the deeper the liquid-jet exit is submerged, the greater the jet mass flow rate will be (see section BACKGROUND) and the quicker the liquid will fill the crevice between the convex end and the side wall of the tank.

The increasing liquid circulation time with decreasing tank filling should significantly affect the rate of bulk-liquid mixing. However, comparing the data for tests 11, 61, and 88 reveals only a slight increase in bulk-liquid mixing times for tank fillings that increase from 32 to 74 percent. The three tests were conducted in the unbaffled

Centaur model tank at nearly identical inflow conditions. The conclusion to be drawn from the data is that, for flow pattern IV and increasing tank bulk-liquid levels, the reduced liquid circulation times and increasing liquid-jet mass flow rates compensated for the additional volume of bulk liquid. Therefore, little effect of tank filling on the bulk-liquid mixing time was observed.

The test results obtained with the 8-centimeter-long jet exit tube at tank liquid fillings of approximately 30 and 50 percent fall into line with the earlier discussions of liquid-jet phenomena. When a liquid jet exits above the liquid-vapor interface, it has a higher velocity and a lower mass flow rate than a submerged jet. Thus, since a significant volume of liquid is required to fill the crevice between the side walls and the concave end of the Centaur model tank, liquid circulation times were greater for the lower mass-flow-rate liquid jet.

Only the data obtained with the 8-centimeter-long jet exit tube and nominal tank liquid fillings of 70 percent did not fit the rationale thus far presented. For these tests the jet exit was only slightly submerged so that little dissipation of the jet was anticipated, but the thin layer of liquid over the jet exit caused it to become irregular in cross section with a pulsating flow characteristic. When this irregular, pulsating jet struck the concave end of the Centaur model tank, splashing resulted rather than the relatively smooth flow that was observed for the other test conditions. The liquid jet splashed off the aft end of the tank and immediately wet the tank walls without filling the crevice. Thus, very short liquid circulation times resulted.

Some splashing was also observed for the tests conducted at tank liquid fillings of approximately 30 percent with the 1-centimeter-long jet exit tube. For these test conditions the layer of liquid over the jet exit was also quite thin and an irregular pulsating jet resulted. However, in contrast to the high-filling-level, 8-centimeter-long jet-exit-tube tests, the splashing was not sufficient to wet the much greater tank wall surface area associated with the lower liquid filling. Complete liquid circulation did not take place until the crevice between the side wall and the convex end of the tank was filled and liquid flowed down the tank wall in an orderly manner.

Baffled Centaur model tank. - The effect of including slosh baffles in the Centaur model tank is shown in figure 15. After 1.8 seconds of inflow the circulating liquid reached the upper baffle (fig. 15(b)); 1.3 seconds later (fig. 15(c)) the liquid had just begun to flow over the slosh baffle. Four tests (7, 35, 58, and 83) exhibited a flow phenomenon similar to that shown in figure 15. Since no appreciable liquid flow was detected on the tank walls below the upper slosh baffle, no attempt was made to extrapolate the data to obtain an analytical determination of the complete liquid circulation time. Under these flow conditions the upper slosh baffle could cause the liquid to collect in the aft end of the experiment tank (liquid flow pattern III). However, it is the

author's belief that the slosh baffles only impede the formation of the complete liquid circulation pattern and this leads to longer circulation times.

Convex hemispherically ended tank. - All the data and extrapolated results of the liquid-circulation-time analysis for the tests with nominally 50-percent liquid fillings are plotted in figure 16. The liquid circulation flow pattern is most rapidly established in tank shape A (convex hemispherically ended), and significantly the position of the jet outlet has a negligible effect on the circulation time. Evidently the liquid-jet momentum, which is essentially the same for both jet outlet positions, is the important parameter for determining the circulation time in a tank with a "clean" configuration.

CONCLUDING REMARKS

This experimental program was conducted to study liquid flow patterns that result from the use of axial jet mixers in partially filled tanks under weightless conditions. The ultimate use of this information is for the design of thermodynamic vent systems that incorporate liquid-jet mixers to provide effective cryogenic-propellant-tank pressure control. Unsubmerged axial liquid jets that provide complete liquid circulation within the tank should prove most effective. Submerged axial jets that provide complete liquid circulation could yield unsymmetric and irregular flow conditions that would place excessive demands on vehicle attitude-control systems. Submerged axial jets for providing only bulk-liquid mixing do appear promising, but the question of adequate pressure control persists.

Before the test results presented in this report can be applied to real space-vehicle cryogenic storage tanks, scaling criteria must be established. The range of acceptable unsubmerged-liquid-jet inflow rates as a function of tank size must be determined so that the undesirable liquid flow conditions (collection or recirculation) can be avoided. The problem of using axial liquid jets to mix the contents of nearly full tanks will persist for any tank size or configuration where the vapor bubble can separate from the tank wall and possibly drift over the mixer inlet.

SUMMARY OF RESULTS

An experimental program was conducted in the NASA Lewis Research Center's 5-second zero-gravity facility to examine the liquid flow patterns that resulted from the axial jet mixing of ethanol in cylindrical (10-cm diam) containers in weightlessness. Several tests were also conducted under normal-gravity conditions for comparison.

Three cylindrical tank configurations were used for the study: a convex hemispherically ended container and two Centaur liquid-hydrogen-tank models, one with slosh baffles and one without. How the liquid volume in the tank; the length of the

0.4-centimeter diameter tube from which the liquid jet exited; and the liquid-jet volumetric flow rate, or average jet velocity, affected the liquid flow patterns was examined.

Four distinct liquid flow patterns were observed during the testing under weightless conditions:

(1) Pattern I - dissipation of the liquid jet in the bulk-liquid region

(2) Pattern II - geyser formation

(3) Pattern III - collection of the jet liquid in the aft end of the tank (opposite jet exit)

(4) Pattern IV - liquid circulation over the aft end of the tank and down the tank wall

For each tank configuration, increasing the liquid-jet average velocity, under weightless conditions, caused a transition from pattern I to pattern IV in succession. Increasing the liquid depth above the jet outlet (increased tank liquid filling) had very little effect on these transition points. Raising the liquid-jet outlet to above the liquid-vapor interface in zero gravity yielded only flow patterns III and IV. For these unsubmerged liquid jets, the transition from pattern III to pattern IV occurred at much lower liquid-jet average velocities in the convex hemispherically ended tank than in the Centaur model tanks.

The results from a few of the zero-gravity tests do not fit into the previously discussed flow pattern classifications. At the higher jet inlet velocities the liquid flow pattern occasionally became irregular, with bubbles being formed, or the liquid flow down the tank wall was entrained by the liquid jet so that the liquid recirculated in the ullage region of the tank. In addition, for tank fillings of 90 percent and greater, there was a tendency for the ullage bubble to become detached from the tank wall, and unsymmetric liquid flow developed.

The time required, after the start of liquid-jet inflow, for complete bulk-liquid mixing and liquid circulation (flow pattern IV) was either measured or extrapolated from the data for each test. Flow pattern I extended to much higher liquid-jet velocities under normal-gravity conditions than zero gravity, and the bulk mixing times were less for a given jet inflow rate in all three test tanks.

The complete liquid circulation times under weightless conditions in the Centaur model tanks were reduced as the liquid-jet average velocity and/or tank filling was increased and were significantly affected by the position of the jet exit tube relative to the liquid-vapor interface. For the Centaur models, at liquid fillings of 50 percent or less - when the liquid jet exited above the liquid-vapor interface - complete liquid circulation times were much greater than those for the submerged jet. At liquid fillings of approximately 70 percent, with the jet outlet centrally located, splashing of the liquid jet off the concave hemispherical end of the Centaur model tanks and onto the tank walls caused the complete liquid circulation times to be very short. For the tests

conducted in the convex hemispherically ended tank the position of the jet outlet had a negligible effect on the resulting circulation times. The addition of a sharp-cornered crevice (tank B) and slosh baffles (tank C) had the effect of increasing liquid circulation times since liquid must fill the corners before circulation can proceed.

For the normal-gravity test conditions, flow pattern II was different from the reduced-gravity data in that the incoming liquid fell back into the bulk region, causing centralized mixing only. Flow pattern IV could only be established with an unsubmerged liquid jet at velocities of nearly 300 centimeters per second.

Lewis Research Center,
National Aeronautics and Space Administration,
Cleveland, Ohio, March 30, 1979,
506-21.

APPENDIX - DATA ACQUISITION

Test Facility

The data for this study were obtained in the 5- to 10-second zero-gravity facility at Lewis. A schematic diagram of this facility is shown in figure 17. The facility consists of a concrete-lined 8.5-meter-diameter shaft that extends 155 meters below ground level. A steel vacuum chamber, 6.1 meters in diameter and 143 meters high, is contained within the concrete shaft. The pressure in this vacuum chamber is reduced to 13.3 newtons per square meter by using the Center's wind tunnel exhaust system and an exhauster system located in the facility.

The ground-level service building has, as its major elements, a shop area, a control room, and a clean room. Assembly, servicing, and balancing of the experiment vehicle are accomplished in the shop area. Tests are conducted from the control room (see fig. 18), which contains the exhauster control system, the experiment vehicle predrop checkout and control system, and the data retrieval system.

Mode of operation. - The zero-gravity facility has two modes of operation. One is to allow the experiment vehicle to free-fall from the top of the vacuum chamber, which results in nominally 5 seconds of free-fall time. The second mode is to project the experiment vehicle upward from the bottom of the vacuum chamber by a high-pressure pneumatic accelerator located on the vertical axis of the chamber. The total up-and-down trajectory of the experiment vehicle results in nominally 10 seconds of free-fall time. The 5-second mode of operation was used for this experimental study.

In either mode of operation the experiment vehicle falls freely; that is, no guide wires, electrical lines, and so forth are connected to the vehicle. Therefore, the only force (aside from gravity) acting on the freely falling experiment vehicle is due to residual air drag. This results in an equivalent gravitational acceleration acting on the experiment which is estimated to be no greater than 10^{-5} g.

Recovery system. - After the experiment vehicle has traversed the total length of the vacuum chamber, it is decelerated in a 3.6-meter-diameter, 6.1-meter-deep container which is located on the vertical axis of the chamber and filled with small pellets of expanded polystyrene. The deceleration rate (averaging 32 g's) is controlled by the flow of pellets through the area between the experiment vehicle and the wall of the deceleration container. This deceleration container is mounted on a cart that can be retracted when using the 10-second mode of operation. In this mode of operation the cart is deployed after the experiment vehicle is projected upward by the pneumatic accelerator. The deceleration container mounted on the cart is shown in figure 19.

Experiment Vehicle

The experiment vehicle consisted of two basic sections (see fig. 20). An experiment section, which is housed in a cylindrical midsection, and a telemetry section, which is contained in the top fairing.

Experiment. - The experiment section consisted of the test container tray plus electrical power and control system equipment mounted in the cylindrical section of the experiment vehicle (fig. 21). The test container tray included the test container, camera, and lighting and timing systems. The liquid flow system, which included an electric drive motor, speed reducing gears, and the piston pump, was mounted below the test container. During the test drop, electric power activated the drive motor and piston pump. The ensuing liquid flow pattern was recorded by a high-speed motion-picture camera. Elapsed time was obtained from a digital clock.

Telemetry system. - The on-board telemetry system is an FM/FM system with 18 continuous channels. During a test drop, telemetry is used to continuously record the position of the piston pump, two low-gravity accelerometers, and other parameters pertinent to the experiment operation.

Test Procedure

The test containers were cleaned in the facility's clean room (fig. 22). The test cylinders were cleaned ultrasonically in a detergent-water solution, rinsed with a distilled-water-methanol solution and dried in a warm air dryer. The test cylinders were then mounted on the test container tray and filled to the desired liquid depth. Contamination of the liquid and cylinder, which could alter the surface tension and contact angle, was carefully avoided. During the test, a predetermined time increment was allowed so that the liquid-vapor interface could approach its low-gravity equilibrium shape. After the formation time, the piston pump was activated, by electric timers, for approximately 3 seconds.

The experiment vehicle is balanced about its vertical axis to ensure an accurate drop trajectory. The vehicle is then positioned at the top of the vacuum chamber as shown in figure 23. It is suspended by the support shaft on a hinged-plate release mechanism. During vacuum chamber pumpdown and before release, monitoring of experiment vehicle systems is accomplished through an umbilical cable attached to the top of the support shaft. Electrical power is supplied from ground equipment. The system is then switched to internal power a few minutes before release. The umbilical cable is remotely pulled from the support shaft 0.5 second before release. The vehicle is released by pneumatically shearing a bolt that holds the hinged plate in the closed

position. No measurable disturbances are imparted to the experiment vehicle by this release procedure.

The total free-fall test time obtained in this mode of operation is 5.16 seconds. During the drop, the vehicle's trajectory and deceleration are monitored on closed-circuit television. After the drop, the vacuum chamber is vented to the atmosphere and the experiment vehicle is returned to ground level.

REFERENCES

1. Lacovic, Raymond F.; et al.: Management of Cryogenic Propellants in a Full-Scale Orbiting Space Vehicle. NASA TN D-4571, 1968.

2. Stark, J. A.; and Blatt, M. H.: Cryogenic Zero Gravity Prototype Vent System. (GDC-DDB67-006, General Dynamics Convair; NASA Contract NAS8-20146.) NASA CR-98079, 1967.

3. Bullard, B. R.: Liquid Propellant Thermal Conditioning System Test Program. (LMSC-D159262, Lockheed Missiles and Space Co.; NASA Contract NAS3-12033.) NASA CR-72971, 1972.

4. Aydelott, John C.: Axial Jet Mixing of Ethanol in Spherical Containers During Weightlessness. NASA TM X-3380, 1976.

5. Poth, Louis J.; and Van Hook, James R.: Control of the Thermodynamic State of Space-Stored Cryogens by Jet Mixing. J. Spacecr. Rockets, vol. 9, no. 5, May 1972, pp. 332-336.

6. Berenyi, Steven G.; Nussle, Ralph C.; and Abdalla, Kaleel L.: An Experimental Investigation of the Effect of Gravity on a Forced Circulation Pattern in Spherical Tanks. NASA TN D-4409, 1968.

7. Schlichting, Hermann (J. Kestin, transl.): Boundary Layer Theory. Sixth ed. McGraw-Hill Book Co., Inc., 1968.

8. Symons, Eugene P.; and Staskus, John V.: Interface Stability During Liquid Inflow to Partially Full, Hemispherical-Ended Cylinders During Weightlessness. NASA TM X-2348, 1971.

TABLE I. - SUMMARY OF TEST PARAMETERS AND RESULTS

Test	Tank shape	Gravity level, g's	Liquid filling, percent by volume	Jet exit tube length, cm	Jet flow rate		Jet average velocity, cm/sec	Liquid flow pattern	Bulk mixing time, sec	Complete-circulation time, sec
					cm^3/sec	Percent of tank volume per test				
1	C	0	29	1	3.0	0.7	24	I	14.5	---
2	C				4.3	1.0	34	II	-----	---
3	C				6.2	1.5	50	III	-----	---
4	B				8.6	2.1	69	IV	-----	3.8
5	C		31		8.5	2.1	68		-----	---
6	B		30		11.9	2.9	95		-----	2.4
7	C		31		11.9	2.9	95		-----	---
8	B		30		13.5	3.3	108		-----	1.9
9			30		16.9	4.1	135		-----	1.7
10			31	8	16.9	4.1	135		-----	4.3
11			32	1	24.2	5.9	193		3.0	1.2
12			29	8	24.3	5.9	194		-----	2.3
13	C		50	1	2.1	.5	17	I	-----	---
14	C	1	52		2.1	.5	17		11.2	---
15	B	0	51		3.0	.7	24		-----	---
16	C	0	51						22.0	---
17	C	1	51						11.6	---
18	A	0	52	8				III/IV	-----	---
19	C	0	52	1	4.3	1.0	34	I	17.5	---
20	C	1	52	1				I	6.9	---
21	A	0	53	8				IV	-----	5.5
22	B		51	8				III	-----	---
23	C		52	8	4.2		33	III	-----	---
24	A		52	1	6.3	1.5	50	II	-----	---
25	C		51	1	6.1	1.5	49	II	-----	---
26	C	1	51	1		1.5		I	5.3	---
27	A	0	56	8		1.4		IV	-----	4.0
28	B	0	51			1.5		III	-----	---
29	B	1	52					I/II	-----	---
30	C	0	51					III	-----	---
31	C	1	52					I/II	-----	---
32	A	0	52	1	8.8	2.1	70	IV	-----	2.6
33	B	0	51		8.5		68	IV	-----	2.9
34	B	1	52		8.5		68	I	4.4	---
35	C	0	51		8.6		69	IV	-----	---
36	C	1	52		8.6		69	I	4.2	---
37	A	0	58	8	8.9		71	IV	-----	2.0
38	B		51	8	8.5		68	III	-----	---
39	C		52	8	8.5		68	III	-----	---
40	A		50	1	12.5	3.0	100	IV	7.5	1.5
41	A	1	52		12.5	3.0	100	I	3.1	---
42	B	0	51		11.8	2.9	94	IV	-----	1.6
43	B	1	51		11.8		94	I	3.6	---
44	C	0	51		11.9		95	IV	-----	2.1
45	C	1	52		11.9		95	I	3.5	---
46	A	0	53	8	11.5	2.7	92	IV	-----	1.8
47	A	1	52		11.5	2.7	92	I/II	-----	---
48	B	0	51		11.8	2.9	94	III	-----	---
49	C	0	52		11.9	2.9	95	III	-----	---

TABLE I. - Concluded.

Test	Tank shape	Gravity level, g's	Liquid filling, percent by volume	Jet exit tube length, cm	Jet flow rate		Jet average velocity, cm/sec	Liquid flow pattern	Bulk mixing time, sec	Complete-circulation time, sec
					cm^3/sec	Percent of tank volume per test				
50	C	1	52	8	11.9	2.9	95	I/II	----	---
51	A	0	52	1	16.8	4.0	134	IV	3.9	.9
52	B	0	51	↓	17.1	4.2	137	IV	3.7	1.1
53	B	1	51	↓	17.1	4.2	137	I	3.2	---
54	C	0	52	↓	16.6	4.1	133	IV	4.2	1.3
55	A	0	53	8	16.6	3.9	133	IV	----	1.0
56	B	0	51	↓	17.0	4.2	136	IV	----	2.3
57	B	1	51	↓	17.0	4.2	136	II	----	---
58	C	0	52	↓	17.0	4.2	136	IV	----	---
59	A	0	52	1	23.4	5.5	187	IV	3.0	.6
60	A	1	52	↓	24.2	5.7	193	I	3.0	---
61	B	0	52	↓	24.0	5.9	192	IV	3.2	.7
62	B	1	51	↓	24.0	5.9	192	I	2.4	---
63	C	0	51	↓	23.4	5.7	187	IV	3.6	1.0
64	C	1	51	↓	23.4	5.7	187	I	2.4	---
65	A	0	55	8	24.4	5.8	195	IV	----	.6
66	B	0	52	↓	24.3	5.9	194	IV	----	1.6
67	B	1	51	↓	24.3	5.9	194	II	----	---
68	C	0	52	↓	22.0	5.4	176	IV	----	2.0
69	C	1	↓	↓	22.0	5.4	176	II	----	---
70	A	0	↓	1	35.4	8.4	283	IV	----	.4
71	↓	1	↓	1	↓	↓	283	II	----	---
72	↓	0	↓	8	↓	↓	283	IV	----	.3
73	↓	1	↓	↓	↓	↓	283	↓	2.9	.4
74	B	0	↓	↓	35.8	8.7	286	↓	6.0	1.0
75	B	1	51	↓	35.8	8.7	286	↓	1.8	.4
76	B	0	73	1	3.0	.7	24	I	----	---
77	C	↓	72	↓	3.0	.7	24	↓	----	---
78	B	↓	73	↓	4.3	1.0	34	↓	23.5	---
79	C	↓	73	↓	4.3	1.0	34	↓	----	---
80	B	↓	73	↓	6.0	1.5	48	II	----	---
81	C	↓	69	↓	6.0	1.5	48	II	----	---
82	B	↓	73	↓	8.5	2.1	68	IV	----	2.2
83	C	↓	73	↓	8.5	2.1	68	↓	----	---
84	B	↓	73	↓	11.9	2.9	95	↓	----	1.4
85	C	↓	72	↓	12.2	3.0	98	↓	----	---
86	B	↓	74	↓	16.9	4.1	135	↓	5.0	.9
87	B	↓	74	8	17.4	4.2	139	↓	7.1	.5
88	B	↓	74	1	23.9	5.8	191	↓	3.3	.5
89	C	↓	75	1	23.4	5.7	187	↓	4.1	.9
90	B	↓	74	8	24.2	5.9	194	↓	----	.3
91	B	↓	91	1	2.2	.5	18	I	----	---
92	C	↓	92	1	6.1	1.5	49	II	----	---
93	B	↓	↓	↓	8.5	2.1	68	IV	----	---
94	C	↓	↓	↓	8.5	2.1	68	↓	----	---
95	B	↓	↓	↓	11.6	2.8	93	↓	----	---
96	C	↓	90	↓	10.5	2.6	84	↓	----	---

TABLE II. - RESULTS OF ZERO-GRAVITY BULK MIXING ANALYSIS

Test	Liquid filling, percent by volume	Jet flow rate, percent of tank volume per sec	Calculated bulk mixing time, sec	Bulk mixing rate, percent of tank volume per sec	Ratio of bulk mixing rate to jet flow rate
1	29	0.24	14.5	2.0	8.3
16	51	.24	22.0	2.3	9.6
19	52	.34	17.5	3.0	8.8
78	73	.34	23.5	3.1	9.1

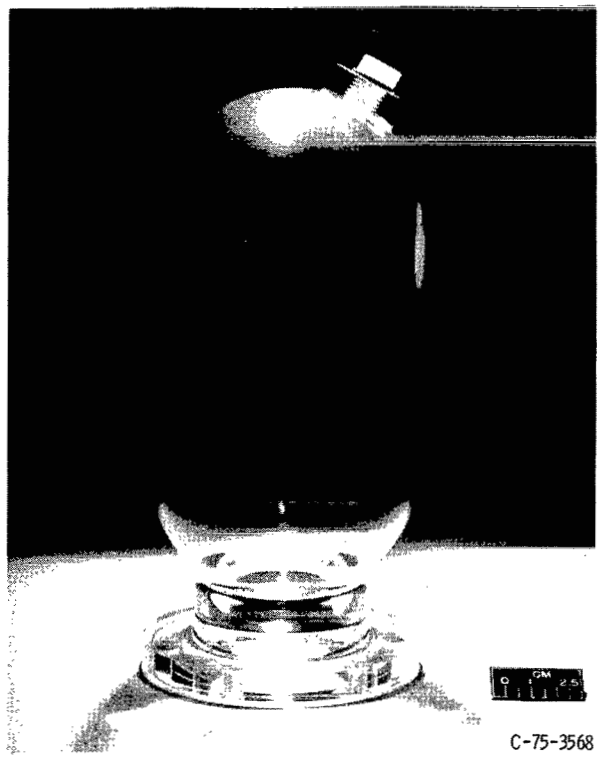

(a) Cylindrical tank with convex hemispherical ends.

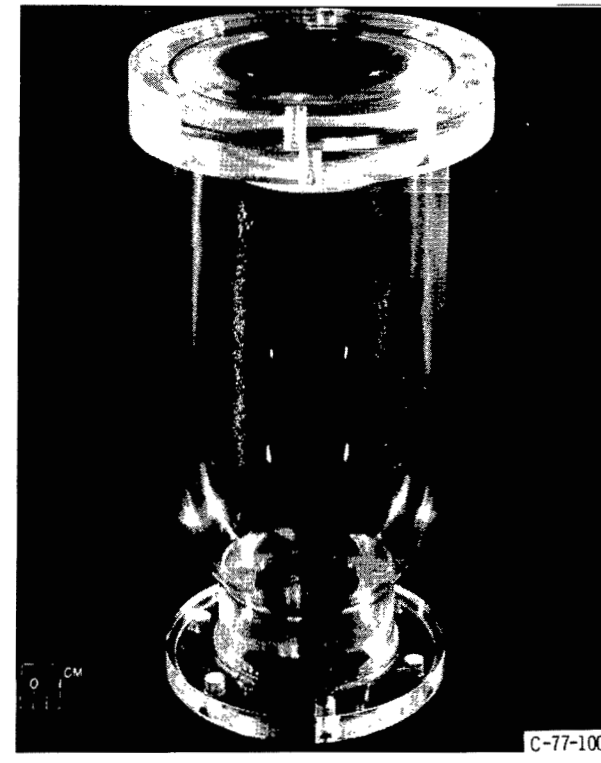

(b) Centaur liquid-hydrogen-tank model without slosh baffles.

Figure 1. - Experiment tanks.

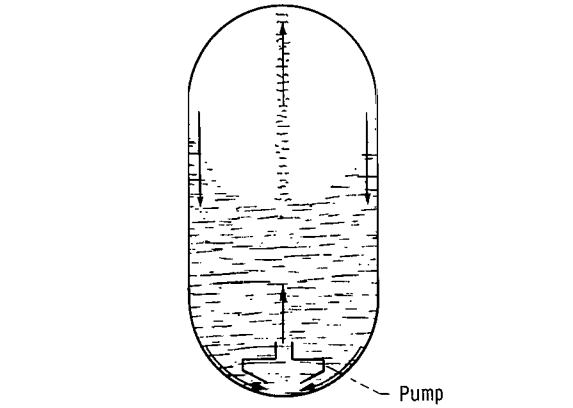

(a) Complete circulation - axial jet.

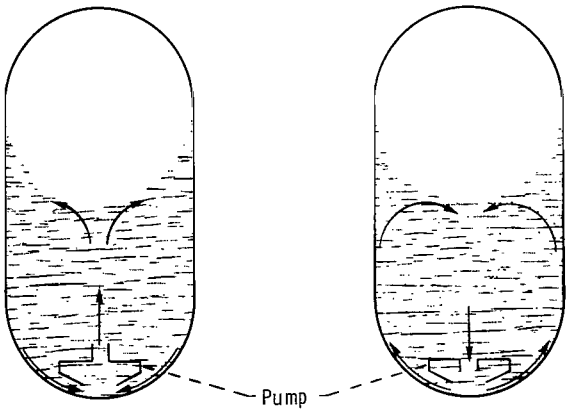

(b-1) Axial jet. (b-2) Radial jet.

(b) Dissipation of liquid jet in bulk-liquid region.

Figure 2. - Liquid-jet pump flow patterns.

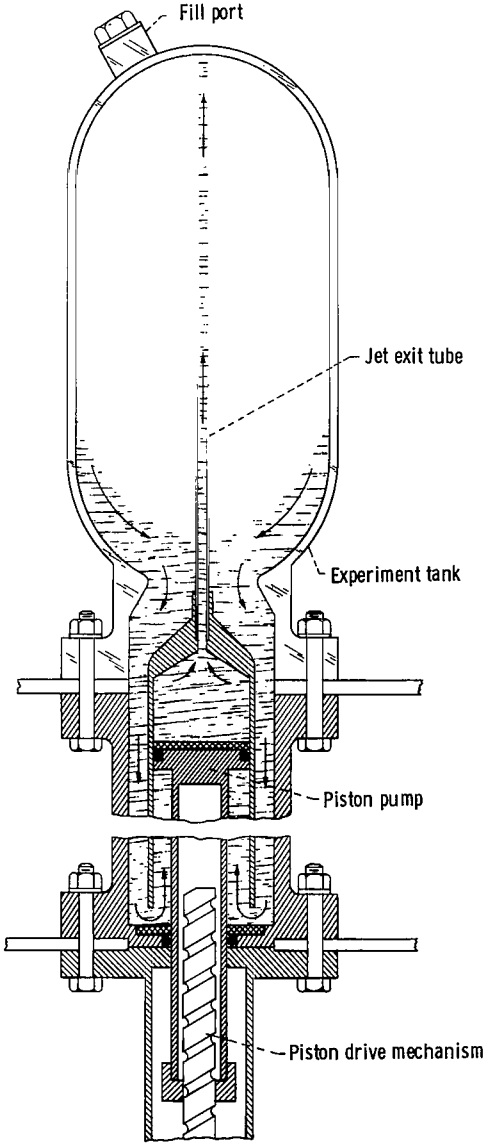

Figure 3. - Liquid flow system.

(a) Test 14 after 1.0 second; jet inflow rate, 0.5 percent.

(b) Test 14 after 2.9 seconds; jet inflow rate, 0.5 percent.

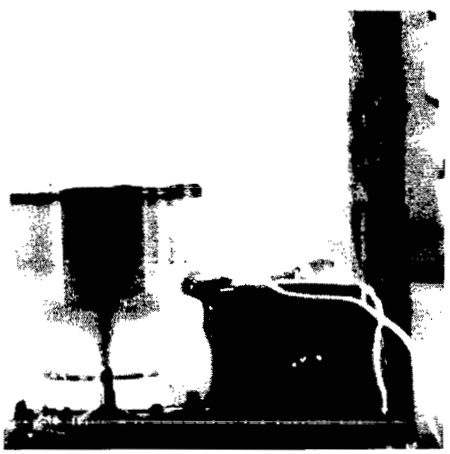

(c) Test 45 after 3.0 seconds; jet inflow rate, 2.9 percent.

Figure 4. - Dissipation of liquid jet in normal gravity. Tests 14 and 45.

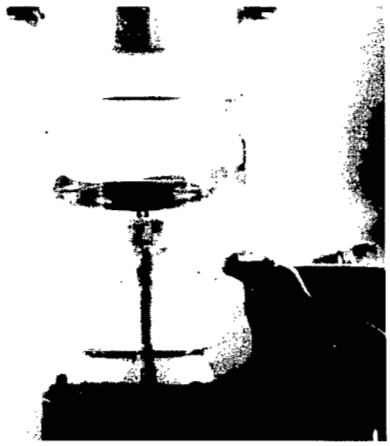

(a) Liquid-jet inflow for 0.3 second.

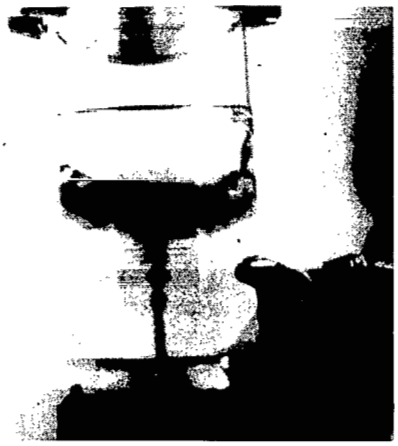

(b) Liquid-jet inflow for 1.5 seconds.

(c) Liquid-jet inflow for 2.9 seconds.

Figure 5. - Dissipation of liquid jet during weightlessness. Test 16; jet inflow rate, 0.7 percent.

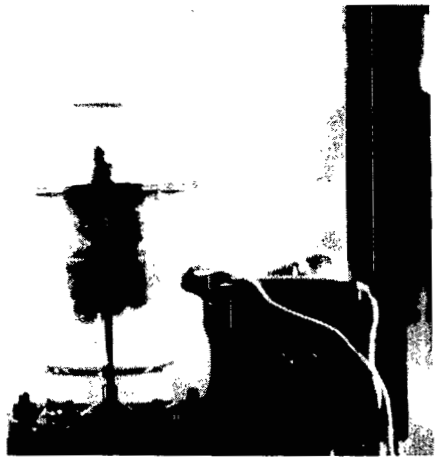

(a) Liquid-jet inflow for 1.0 second.

(b) Liquid-jet inflow for 3.0 seconds.

Figure 6. - Geyser formation in normal gravity. Test 50; jet inflow rate, 2.9 percent.

(a) Liquid-jet inflow for 0.2 second.

(b) Liquid-jet inflow for 2.0 seconds.

(c) Liquid-jet inflow for 3.0 seconds.

Figure 7. - Geyser formation during weightlessness. Test 24; jet inflow rate, 1.5 percent.

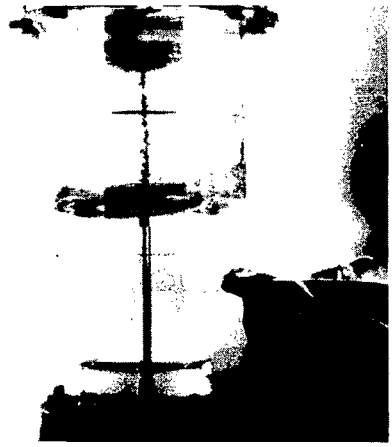

(a) Liquid-jet inflow for 0.5 second.

(b) Liquid-jet inflow for 1.5 seconds.

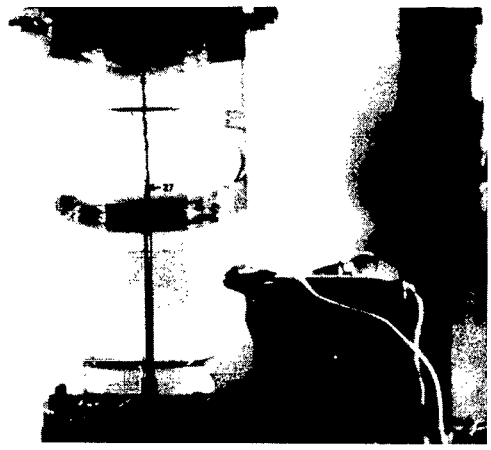

(c) Liquid-jet inflow for 3.1 seconds.

Figure 8. - Liquid collection during weightlessness. Test 49; jet inflow rate, 2.9 percent.

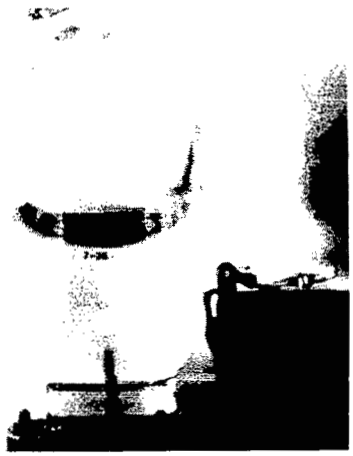

(a) Zero-gravity liquid-vapor interface configuration at start of flow.

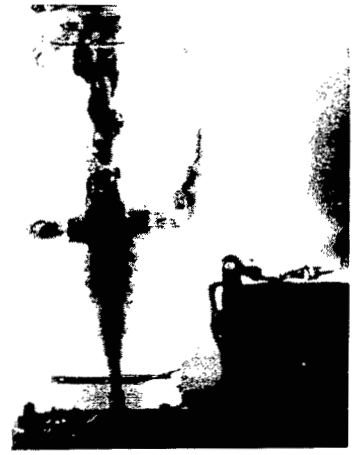

(b) Liquid-jet inflow for 0.5 second.

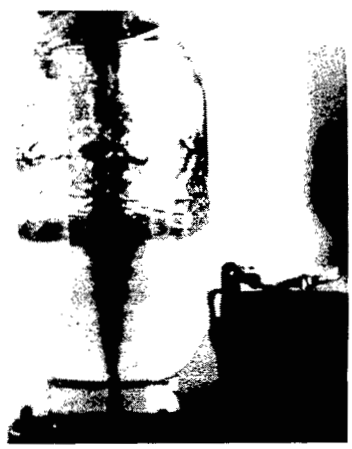

(c) Liquid-jet inflow for 0.8 second.

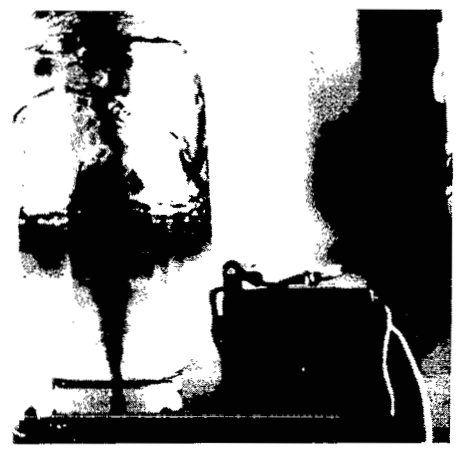

(d) Liquid-jet inflow for 1.5 seconds.

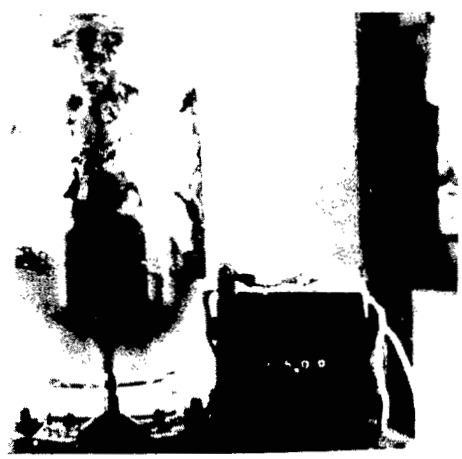

(e) Liquid-jet inflow for 3.1 seconds.

Figure 9. - Liquid circulation during weightlessness. Test 59; jet inflow rate, 5.5 percent.

(a) Liquid-jet inflow for 0.5 second.

(b) Liquid-jet inflow for 1.5 seconds.

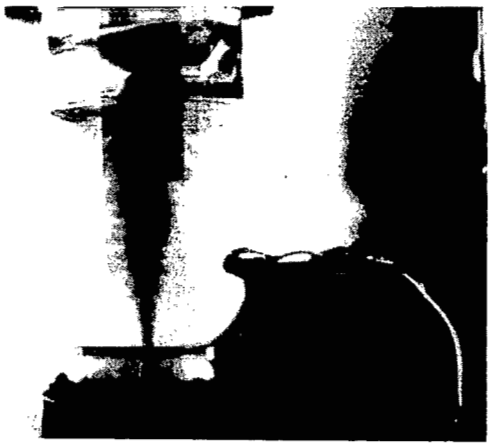

(c) Liquid-jet inflow for 1.8 seconds.

(d) Liquid-jet inflow for 2.5 seconds.

(e) Liquid-jet inflow for 3.1 seconds.

Figure 10. - Unsymmetic liquid circulation during weightlessness. Test 96; liquid filling, 90 percent; jet inflow rate, 2.6 percent.

(a) Liquid-jet inflow for 0.4 second.

(b) Liquid-jet inflow for 1.2 seconds.

(c) Liquid-jet inflow for 3.2 seconds.

Figure 11. - Bubble formation during weightlessness. Test 70; jet inflow rate, 8.4 percent.

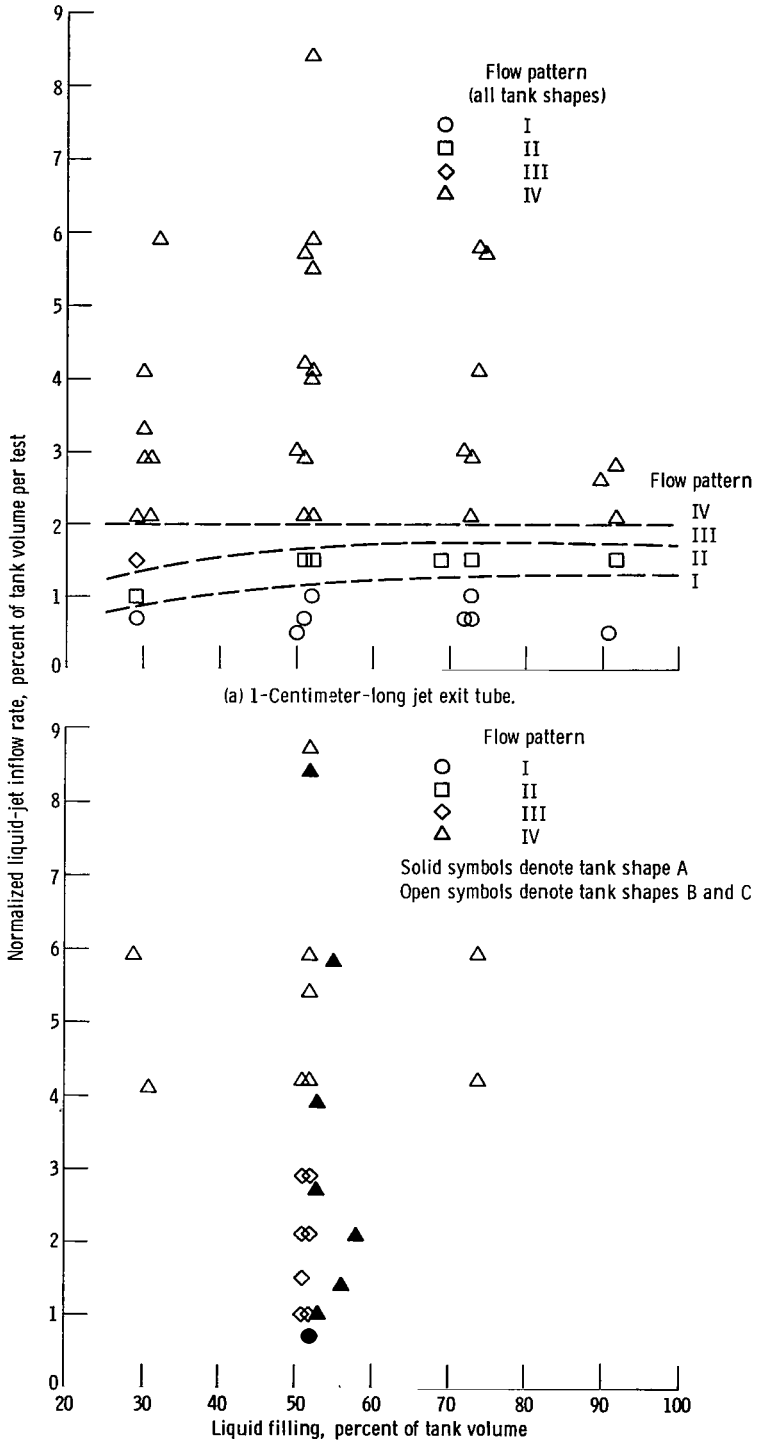

(a) 1-Centimeter-long jet exit tube.

(b) 8-Centimeter-long jet exit tube.

Figure 12. - Liquid flow patterns during weightlessness as function of jet airflow rate, liquid filling, and tank shape.

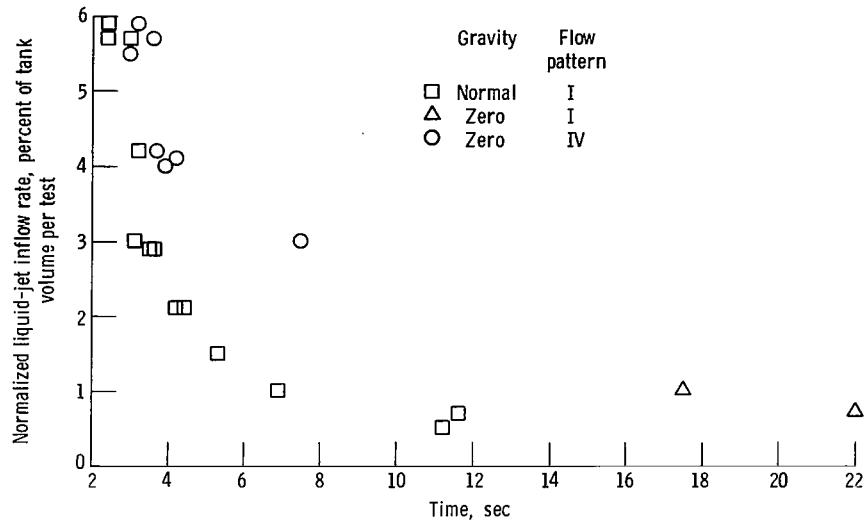

Figure 13. - Bulk-liquid mixing time as function of jet inflow rate and gravity. Nominal liquid filling, 50 percent; jet exit tube length, 1 cm; tank shapes A, B, and C.

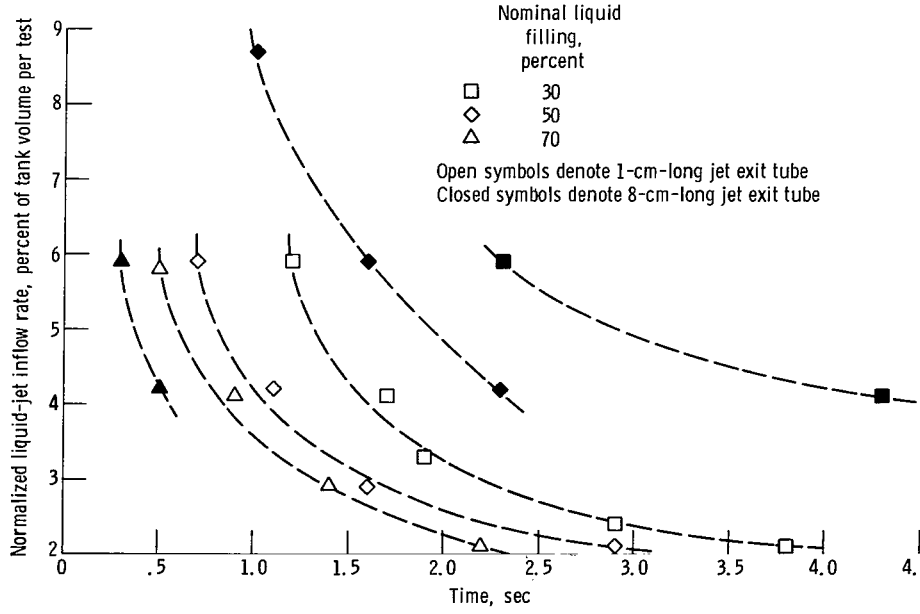

Figure 14. - Liquid circulation time as function of liquid filling, jet exit tube position, and jet inflow rate. Tank shape B.

(a) Zero-gravity liquid-vapor interface configuration at start of flow.

(b) Liquid-jet inflow for 1.8 seconds.

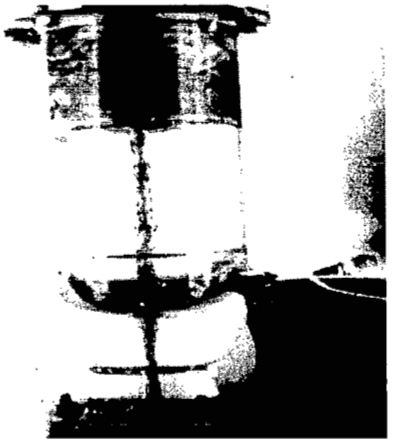

(c) Liquid-jet inflow for 3.1 seconds.

Figure 15. - Effect of slosh baffles on liquid circulation. Test 7; liquid filling, 31 percent; jet inflow rate, 2.9 percent.

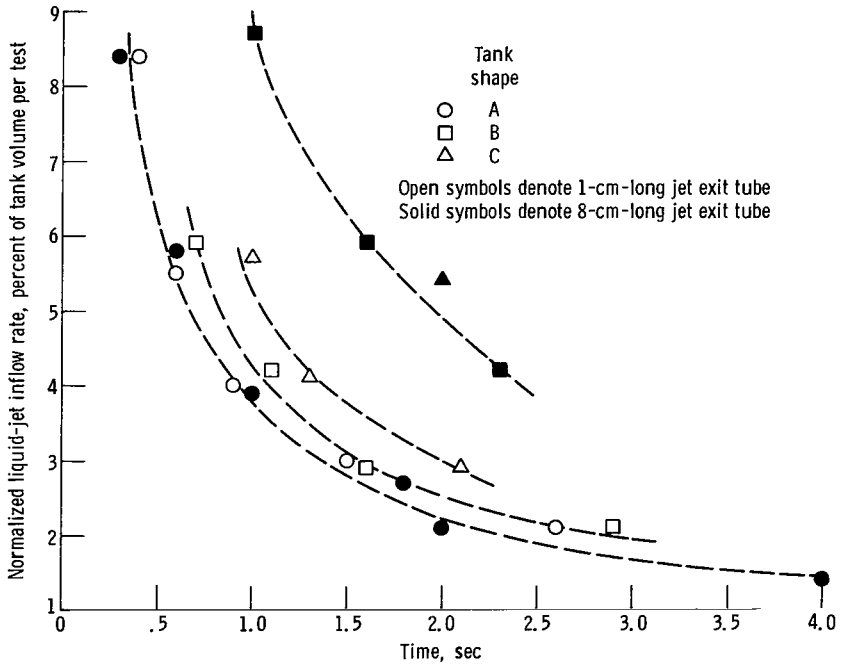

Figure 16. - Liquid circulation time as function of tank shape, jet exit tube position, and jet inflow rate. Nominal liquid filling, 50 percent.

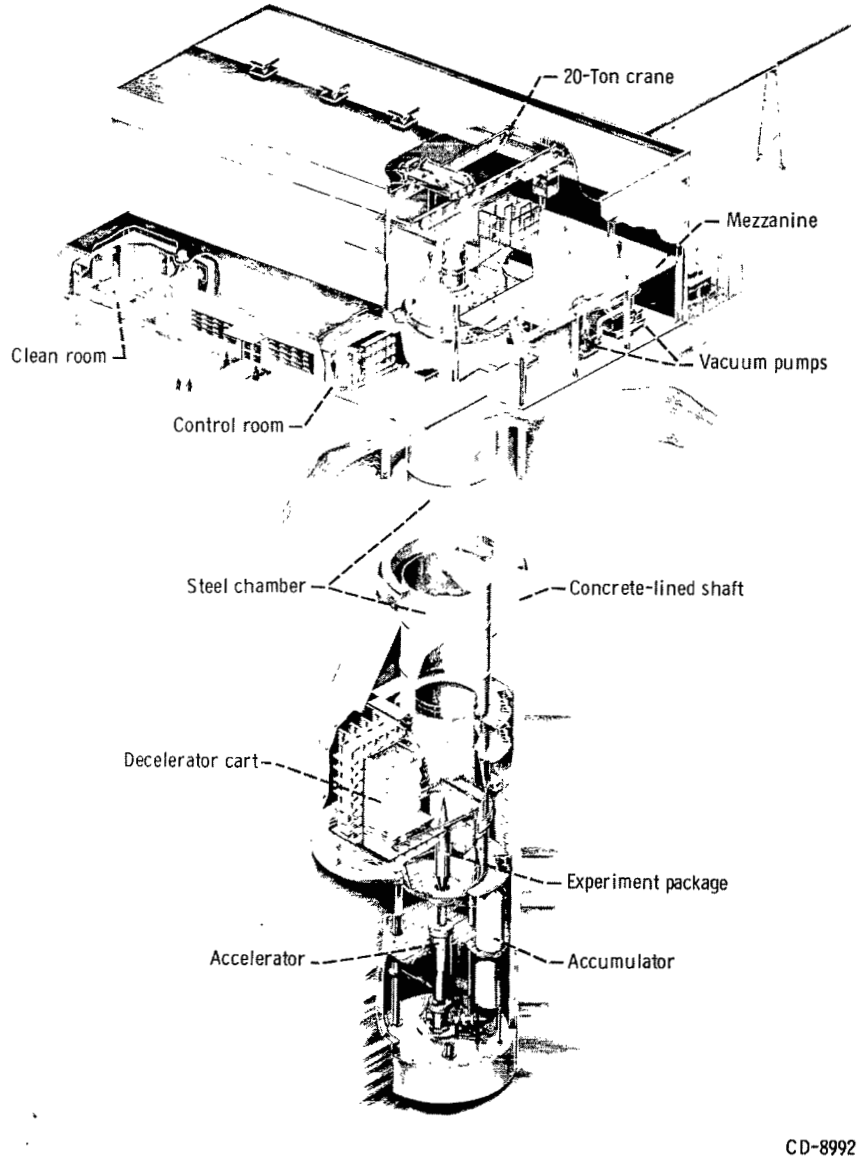

Figure 17. - 5- To 10-second zero-gravity facility.

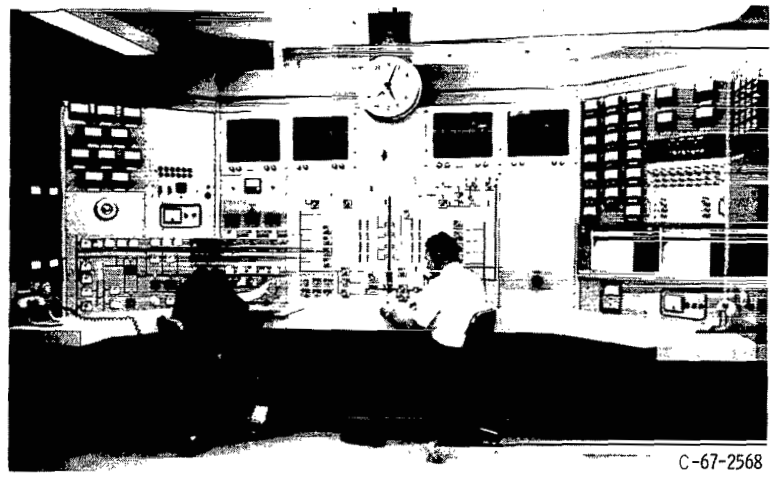

Figure 18. - Control room.

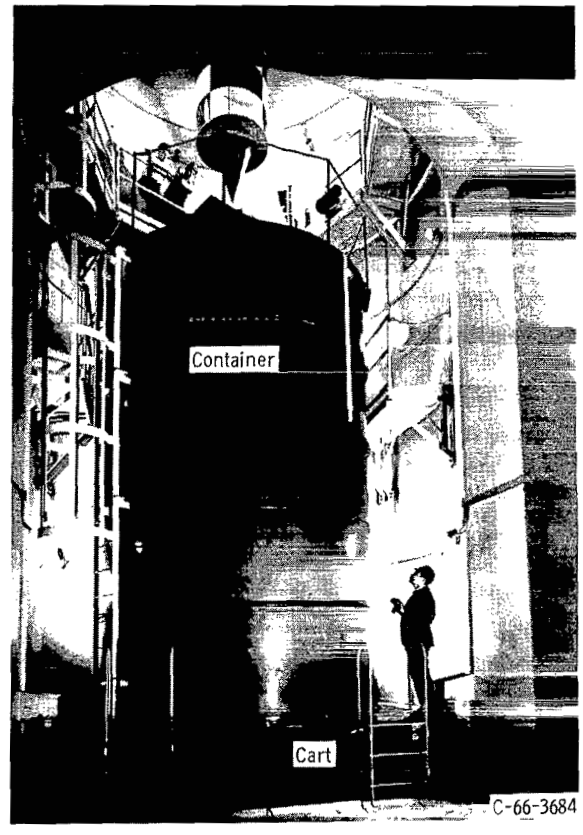

Figure 19. - Deceleration system.

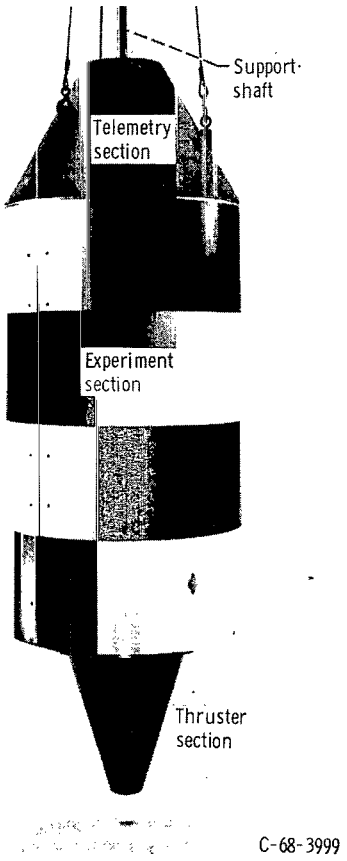

Figure 20. - Experiment vehicle.

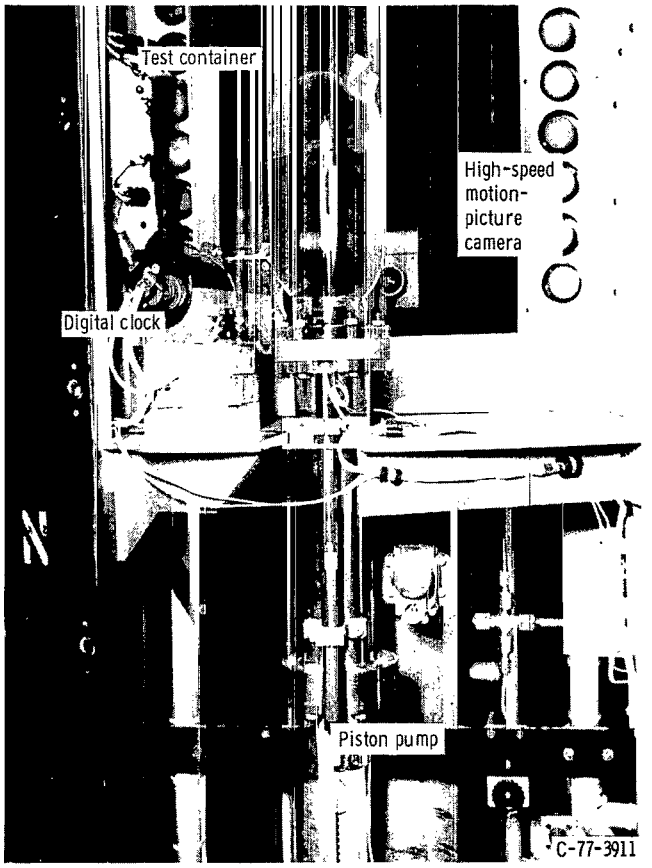

Figure 21. - Experiment section.

Figure 22. - Facility clean room.

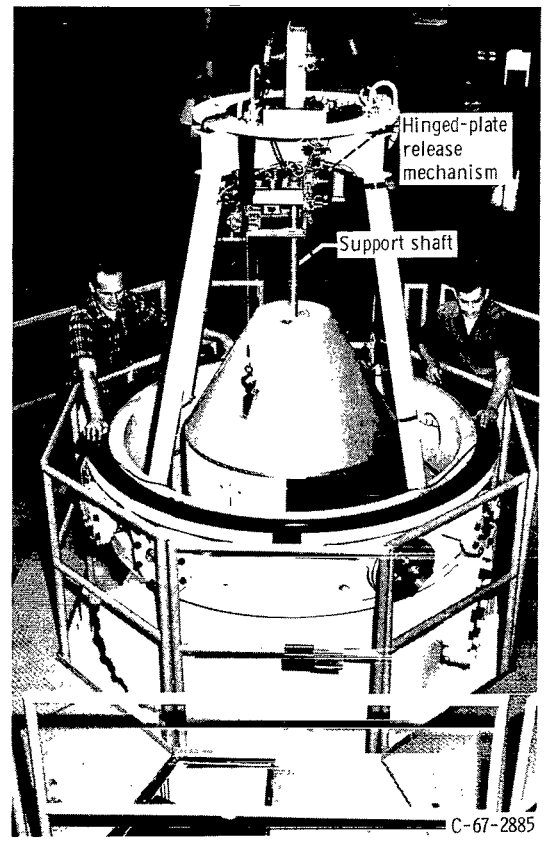

Figure 23. - Vehicle position before release.

1. Report No.	2. Government Accession No.	3. Recipient's Catalog No.
NASA TP-1487		

4. Title and Subtitle	5. Report Date
AXIAL JET MIXING OF ETHANOL IN CYLINDRICAL CONTAINERS DURING WEIGHTLESSNESS	July 1979
	6. Performing Organization Code
7. Author(s)	8. Performing Organization Report No.
John C. Aydelott	E-9937
	10. Work Unit No.
9. Performing Organization Name and Address	506-21
National Aeronautics and Space Administration Lewis Research Center Cleveland, Ohio 44135	11. Contract or Grant No.
	13. Type of Report and Period Covered
12. Sponsoring Agency Name and Address	Technical Paper
National Aeronautics and Space Administration Washington, D.C. 20546	14. Sponsoring Agency Code

15. Supplementary Notes

16. Abstract

An experimental program was conducted to examine the liquid flow patterns that result from the axial jet mixing of ethanol in 10-centimeter-diameter cylindrical tanks in weightlessness. A convex hemispherically ended tank and two Centaur liquid-hydrogen-tank models were used for the study. Four distinct liquid flow patterns were observed to be a function of the tank geometry, the liquid-jet velocity, the volume of liquid in the tank, and the location of the tube from which the liquid jet exited.

17. Key Words (Suggested by Author(s))

Liquid propellants
Fluid dynamics
Axial liquid-jet
Mixing
Weightlessness

18. Distribution Statement

Unclassified - unlimited
STAR Category 28

19. Security Classif. (of this report)	20. Security Classif. (of this page)	21. No. of Pages	22. Price*
Unclassified	Unclassified	42	A03

* For sale by the National Technical Information Service, Springfield, Virginia 22161

NASA-Langley, 1979

National Aeronautics and
Space Administration

Washington, D.C.
20546

Official Business
Penalty for Private U

THIRD-CLASS BULK RATE

Postage and Fees Paid
National Aeronautics and
Space Administration
NASA-451

U.S.MAIL

4 1 1U,C, 072079 S00903DS
DEPT OF THE AIR FORCE
AF WEAPONS LABORATORY
ATTN: TECHNICAL LIBRARY (SUL)
KIRTLAND AFB NM 87117

S

NASA

POSTMASTER: If Undeliverable (Section 158 Postal Manual) Do Not Return